Combining Magnetic Flux Leakage and Optical Inspection Technique for Identification of Nearby Pittings

Turaj Azizzadeh
Department of Mechanical Engineering,
University of Science and Technology, Iran
E-mail: azizzadeh@mecheng.iust.ac.ir

Mir Saeed Safizadeh*
Department of Mechanical Engineering,
University of Science and Technology, Iran
E-mail: safizadeh@iust.ac.ir
*Corresponding author

Received: 19 July 2018, Revised: 23 September 2018, Accepted: 17 December 2018

Abstract: Magnetic Flux Leakage (MFL) is an indirect measurement technique. Therefore, calibration curves are generally used to estimate the depths of the defects from the measured MFL signals. This has been shown to give good results on varying degrees of the single defects. However due to the interaction between the leakage fluxes, nearby pittings can-not be discriminated and properly assessed using the conventional MFL technique. In order to ensure reliable measurement for this case, the MFL technique is combined with the optical inspection technique. The main contributions of this study are to develop a new calibration method based on the defect depth, defect area as well as the amplitude of the corresponding MFL signal and propose a novel combined approach for detection and identification of the nearby pittings. MFL and optical inspection techniques are applied to a test specimen containing the nearby pittings. The results obtained from the experimental tests demonstrate the efficacy of the proposed approach.

Keywords: Magnetic Flux Leakage, Optical Inspection Technique, Pipeline

Reference: Azizzadeh, T., Safizadeh, M. S., "Combining Magnetic Flux Leakage and Optical Inspection Technique for Identification of Nearby Pittings", Int J of Advanced Design and Manufacturing Technology, Vol. 11, No. 4, 2018, pp. 73–80.

Biographical notes: Turaj Azizzadeh is PhD student of Mechanical engineering at the University of Science and Technology, Iran. He received his MSc in Mechanical engineering from University of Science and Technology, Iran and a BSc in Mechanical engineering from the University of Tabriz, Iran. His current research focuses on advanced non-destructive testing techniques. **Mir Saeed Safizadeh** received his PhD in Mechanical Engineering from University of Montreal, Canada, in 1999. He is currently Associate Professor at the Department of Mechanical Engineering, University of Science and Technology, Tehran, Iran. His current research interest includes non-destructive testing techniques.

1 INTRODUCTION

Carbon steel pipelines are widely used to transport invaluable energy resources such as oil and gas over long distances. Pitting corrosions are frequently found in the pipelines and may occur singly or in colonies. Colonies of nearby pittings are hardly found in liquid pipelines due to the corrosion mechanism. These defects are usually found in gas pipelines and increase the likelihood of a leak [1]. Due to the interaction between the defects, nearby pittings reduce the ability of a pipeline to withstand the internal pressure [2]-[4]. Also, these defects increase the corrosion growth rates in the wall of the pipeline [5].

In order to prevent pipeline failure, early detection of the defects is extremely important [6]. Over the years, a number of techniques have been developed for inspection of the pipelines. However, magnetic flux leakage (MFL) and ultrasonic (UT) are two conventional methods for inspection of the pipes [7]. MFL is the most widely used method for inspection of the gas pipelines [8]-[9] while UT generally can-not be used due to the absence of the needed liquid coupling medium [10]-[11]. The MFL technique consists of magnetizing the ferromagnetic pipe wall to the magnetic saturation state and detecting the defect-induced magnetic leakage fields using the magnetic field sensors. A pitting corrosion acts as an area of high magnetic reluctance that causes magnetic flux to leak out of the defect [12]. MFL techniques can characterize most corrosion defects with sufficient accuracy. However, some corrosion geometries such as nearby pittings provide a greater challenge for the traditional MFL technique [13]. This is the problem we addressed in the paper, namely the characterization of the nearby pittings using the MFL technique.

This paper provides insight into why nearby pittings are erroneously sized with MFL technique and proposes a novel solution for this problem. A major contribution of this study is to introduce and investigate a novel approach for decomposing the shapes and depths of the nearby pittings using the combination of MFL and optical inspection data. Also, a new method for calibrating the MFL signals is developed to better estimate the depths of the pittings.

2 LITERATURE REVIEW

The major limitation of the MFL technique is its inability to accurately characterize the nearby pittings. MFL signals are considered to be proportional to the defect volume [14]. So, the MFL signal amplitude is not a direct indicator of the underlying defect depth but is a function of defect depth combined with length and width. Depth of the pittings is the most critical dimension because it increases the likelihood of a leak [15]-[18]. The defect depth can be extracted from the volume, length and width measurements which need calibration work. Although the calibration of the MFL signals in terms of defect depth is abundant in the literature, the MFL relationship to defect area (the length and width of a defect) has been largely overlooked. Taking into account the defect area is helpful to estimate the depth accurately, in particular in case of the nearby pittings. However, the broader MFL signals interfere for nearby pittings which make accurate depth sizing very difficult [19]. In other words, MFL data do not provide a sufficiently detailed resolution to identify distinct corrosion pits in the nearby pittings and this subsequently influences the depth sizing accuracy. This is caused by the nature of the electromagnetic non-destructive testing methods and an urgent solution for this problem is required.

In the past, inspection systems based only on a single technique were used for detection of the defects. Researches have shown that, while single-technique systems can provide useful data, there are also limitations to each type of technique. Considering the variety of the possible defects, single-technique systems (either magnetic or ultrasonic) do not yield sufficient information for accurately characterizing the defects. For this reason, inspection systems utilizing multiple techniques have been suggested to overcome these limitations and to ensure the optimal detection of the defects.

The simultaneous use of multiple techniques provides several advantages compared to the single-technique systems. Looking at the same defect by different datasets gets an increasingly clear picture. These data can be correlated more completely resulting in a reliable analysis and defect identification [20]-[24].

The process of sizing the nearby pittings is a two-step process. First, the MFL data must be partitioned into individual pittings. Second, the individual pittings are sized using the appropriate calibration models. Currently, optical inspection technique is one of the best techniques available for the pipe surface measurement. This technique can inspect the internal surface of the pipelines at a resolution of 1mm or finer and get a high resolution data for defect surface measurement [25]. To overcome the limitations of the MFL, optical inspection technique can be combined with this technique to enable increased discrimination of the individual pittings in colonies of the nearby pittings.

The contribution of this work is twofold. First, a new method for calibrating the MFL signals is developed to better estimate the depths of the pittings. Second, a novel approach based on the combination of MFL and optical inspection data is proposed for decomposing the shapes and depths of the nearby pittings.

3 MFL EXPERIMENT

The MFL experimental setup comprised a magnetizer, a specimen, a controllable scanner, a data acquisition system and other associated units as schematically shown

in "Fig. 1". The Hall-effect sensor was scanned over the surface area of the specimen using a 3-axis scanner. The scanner acquired its movement instructions from a PC, by the parallel port. The scanning region was centralized on the defects geometry and was 1cm on either side of the edges of the defects. The scanning resolution was set to 2mm in both axial and circumferential directions. At every x-y position on the scanning region, the MFL signals were precisely obtained with a gauss meter and recorded on a computer via a USB connection. Throughout all the MFL experiments, the lift-off distance was kept constant equal to 2mm.

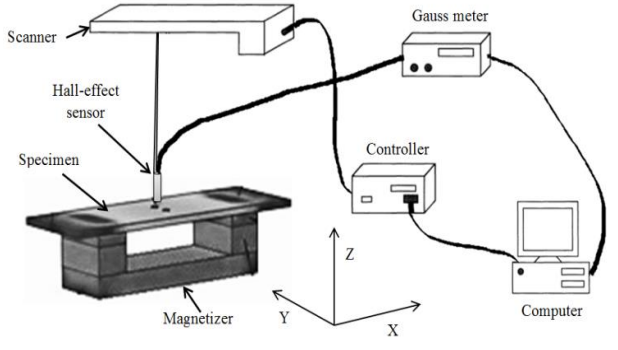

Fig. 1 Schematic of the MFL inspection technique.

Figure 2 shows the photograph of the MFL experimental setup.

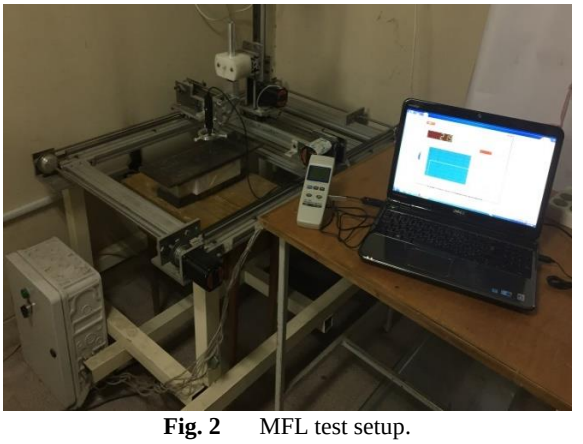

Fig. 2 MFL test setup.

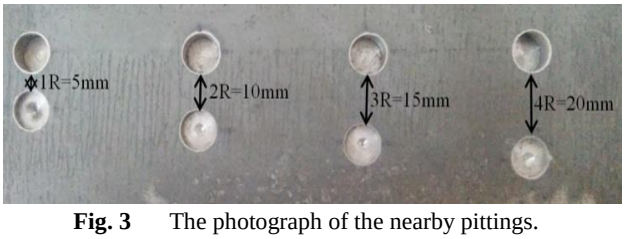

Fig. 3 The photograph of the nearby pittings.

MFL experiments were performed on the X52 steel plate containing a series of machined nearby pittings. The thickness of the steel plate was 10mm. Defects were located at the central area of the specimen. Pitting defects had 10mm diameter and different depths. The work was limited mainly to the interactive type of the pittings vertically aligned to the magnetization direction. The degree of interaction was considered in four patterns according to the edge-to-edge distances between the two nearby pittings. The photograph of the nearby pittings with different edge-to-edge distances are shown in "Fig. 3".

Figure 4 shows the MFL C-scans obtained from the experimental tests. The amplitudes of the MFL signals were normalized in order to obtain a maximum contrast. The solid circles in "Fig. 4" indicate the true positions of the pittings.

The C-scans in "Fig. 4" clearly show the inability of the MFL technique for discriminating the widths of the nearby pittings. As a result, the MFL C-scan might report a wide pitting defect when in actuality the defects are two nearby pittings. This can be explained by the fact that the broader MFL signals interfere with each other, which makes it difficult to discriminate the individual pittings. However, estimation of the defect depth is very sensitive to the width of the defect and a good estimation of the width is essential for proper depth sizing [26]-[27].

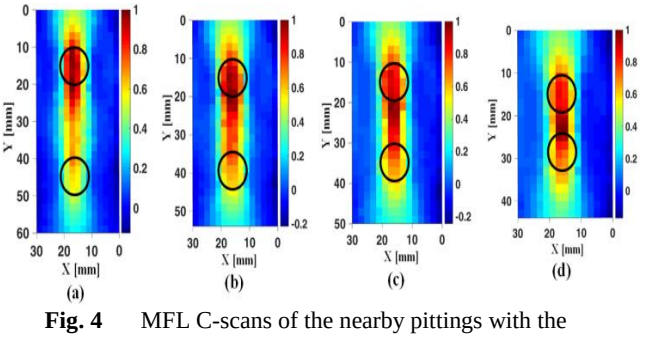

Fig. 4 MFL C-scans of the nearby pittings with the separations of: (a) 4R, (b) 3R, (c) 2R, and (d) 1R, respectively.

4 OPTICAL INSPECTION EXPERIMENT

The optical inspection system comprised a CCD camera, a linear laser diode, and a 3-axis scanner. Camera calibration factors are achieved by a calibration technique suggested by Zhang [28]. The experimental measurement system is shown in "Fig. 5".

During the scanning of the optical inspection system along the surface of the specimen, the laser lines are constantly captured by the camera. By means of a frame grabber, the inspection data were actually stored as a movie. The scanner moved at a constant speed of approximately 0.03 m/s. The recording frequency of the camera was 30 frames/s.

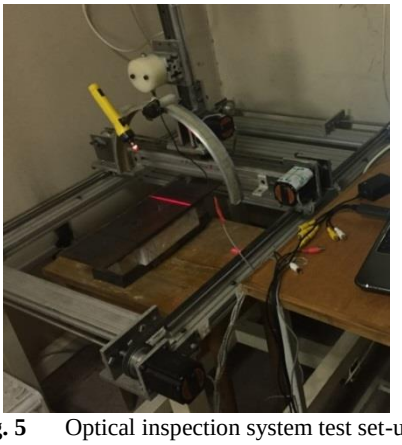

Fig. 5 Optical inspection system test set-up.

For analysing the raw data, MATLAB software and image processing codes were used. First, the frames of the recorded movie were extracted. The image processing techniques including contrast adjustment, median filter, and canny edge detector were implemented to enhance the quality of the images and to detect the edges of the laser lines [29]. The images of the laser lines at the positions of the pittings with different separation distances are shown in "Fig. 6".

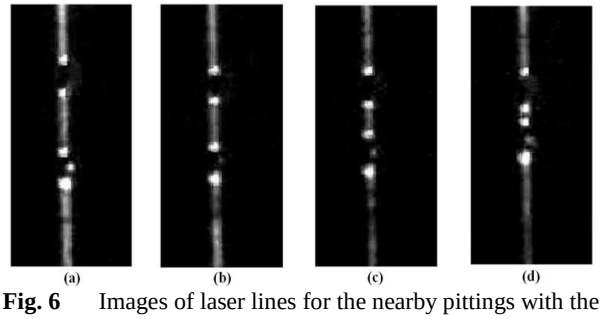

Fig. 6 Images of laser lines for the nearby pittings with the separations of: (a) 4R, (b) 3R, (c) 2R, and (d) 1R, respectively.

After the laser lines were extracted from the background images, an intensity extraction algorithm was applied to the segmented laser lines. The algorithm calculated the mean values of the intensities along the individual segments. Equation (1) was used for computation of the local average intensity. In Eq. (1), μ_j is the local average of segment j, i is the gray level intensity of a certain image point, and the size of the scanning window is $n \times m$.

$$\mu_j = \frac{\sum i}{n \times m} \tag{1}$$

Intensity plot along the laser line passing through the nearby pittings with a 20mm separation distance is shown in "Fig. 7". In this plot, X-axis is circumferential distance onto the laser line in mm and Y-axis is the intensity level.

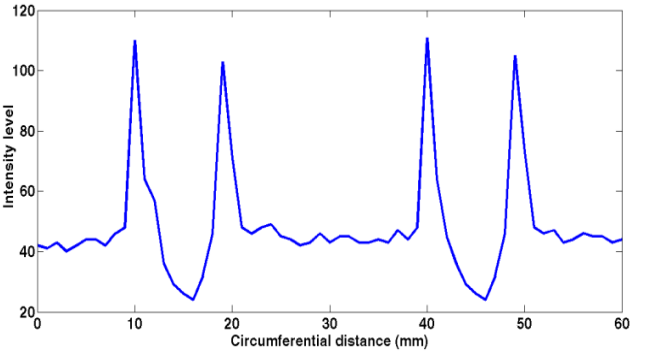

Fig. 7 Laser intensity plot of the nearby pittings with the separation of 4R.

The peaks of the intensities in the above plot show the positions of the pittings onto the laser line. A C-scan image of the nearby pittings is produced from the sequential intensity plots, while the inspection system scans the surface of the plate. C-scan images for the defined defect geometries are shown in "Fig. 8".

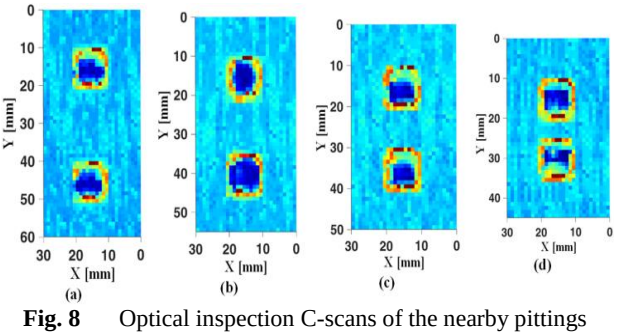

Fig. 8 Optical inspection C-scans of the nearby pittings with the separations of: (a) 4R, (b) 3R, (c) 2R, and (d) 1R, respectively.

In the obtained C-scans, resolutions of 1 mm along the line segments and resolutions of 1 mm in the longitudinal direction were considered. Abrupt changes of the intensities in the circumferential as well as longitudinal directions indicate the positions of the pittings. The main interest here was to identify the pixels where the differences in the intensity levels were high. It was noted that the edges of the pittings were located when using this technique.

Thresholding technique was utilized so that the image was processed in a binary format. Edges of the defects were identified at this step. Low intensity pixels and background pixels were filtered while high intensity pixels were identified as edges. In this step, all the pixels which had a higher intensity than a predefined threshold were identified. These pixels had a high chance of belonging to the defect edges.

Then, a circle fitting algorithm was applied to the identified pixels and edges to estimate the diameters of the pittings (Fig. 9). The results of the diameter estimation compared to the real sizes of the pittings are

given in Table 1. The relative error for diameter estimation is below 6 percent.

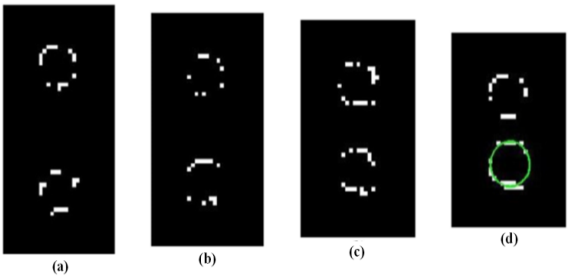

Fig. 9 Fitting the circles to the identified pixels.

Table 1 The results of the diameter estimations for the nearby pittings

The spacing between the pittings	Pitting depth	Pitting diameter (mm)	Diameter estimation error (%)
4R=20mm	80%t	10	-1.3
	30%t	10	-3.3
3R=15mm	80%t	10	-1
	30%t	10	4.5
2R=10mm	80%t	10	-0.6
	30%t	10	-0.5
1R=5mm	80%t	10	-5.4
	30%t	10	0.1

The abrupt changes in the intensities can be related to the geometrical changes of the inspected surface where defects occur and the characteristics of the reflected light at those locations. At the edges of defects, the surface changes from horizontal to oblique and this leads to the variation of the light incidence angle. Since the quantity of the reflected light is proportional to the incidence angle, as a result the reflected light intensity changes, as shown in "Fig. 8".

Although optical inspection data only give the two dimensional profile limited to the length and width of the defect and do not have the capability to give depth information of the pittings, they can still be used to optimize the width sizing accuracy of the nearby pittings. As a result, the depth estimation accuracy of the nearby pittings is improved by combining the information received from the MFL and optical inspection techniques.

5 COMBINATION OF THE MFL AND OPTICAL INSPECTION RESULTS

MFL and optical scanning are different inspection techniques. Each of these two techniques operates utilizing the distinct physical phenomena (magnetic versus optical). In MFL, the leakage fluxes are measured. In optical scanning, the emitted laser intensities are registered while the specimen is scanned by a laser. The separation and sizing of the nearby pittings were carried out using the combined evaluation of the MFL and optical inspection data. In this case, the optical inspection data help the MFL depth estimation algorithm by enabling increased discrimination of the individual pittings. The flowchart for the depth estimation of the nearby pittings is given in "Fig. 10".

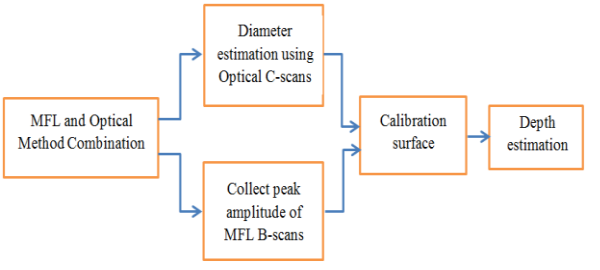

Fig. 10 Steps of the depth estimation for the nearby pittings.

For each technique, the C-scans were evaluated separately and then transferred into a combined evaluation. The C-scans as acquired from the nearby pittings having circumferential distances between 5mm and 20mm clearly showed that optical inspection technique provided a greater discrimination of the shapes of the individual pittings. However due to the blooming effects [30], the MFL signals interfered for circumferential distances < 20mm, which made it difficult to separately identify the individual pittings. This was due to the nature of the electromagnetic non-destructive testing techniques and the morphology of the defects. Thus, the accuracy of the depth estimation may be reduced.

A combined evaluation of the MFL B-scan/C-scan data with the C-scan data of the optical inspection measurements can provide an improved depth estimation of the nearby pittings. In this case, the C-scans of the optical inspection technique were used to segment the MFL data into individual pittings as well as to facilitate the diameter estimation of the pitttings. It is worth mentioning that the MFL data region corresponds to the same physical area of the steel plate scanned by the optical inspection technique.

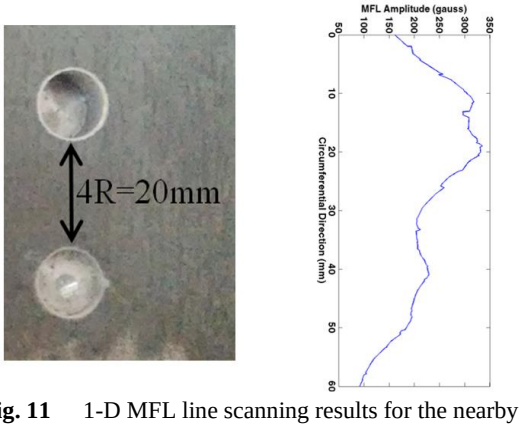

Fig. 11 1-D MFL line scanning results for the nearby pittings with the spacing of 4R.

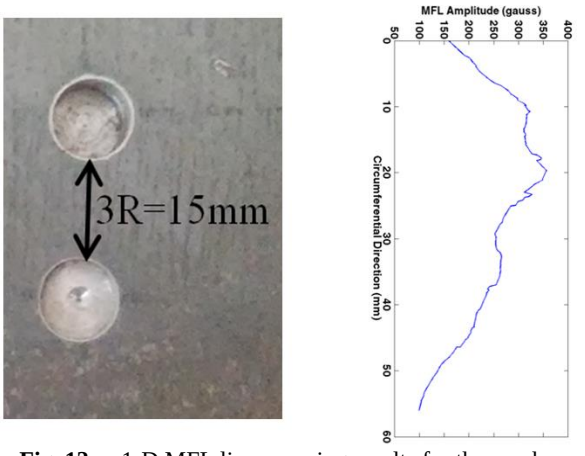

Fig. 12 1-D MFL line scanning results for the nearby pittings with the spacing of 3R.

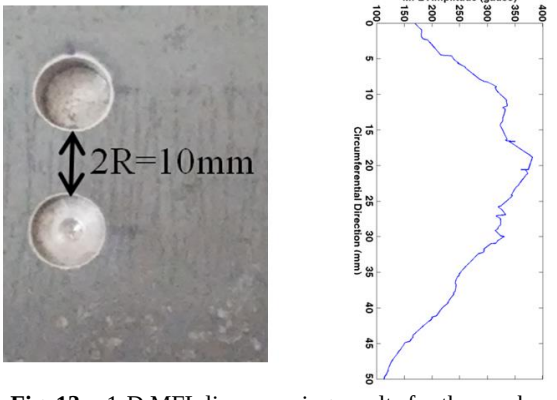

Fig. 13 1-D MFL line scanning results for the nearby pittings with the spacing of 2R.

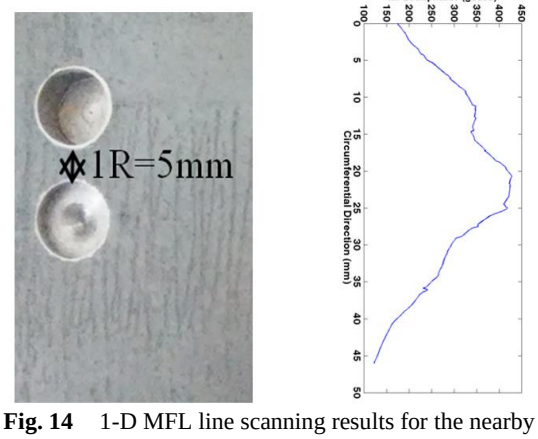

Fig. 14 1-D MFL line scanning results for the nearby pittings with the spacing of 1R.

Figures 11-14 show the photograph of the nearby pittings and the corresponding MFL B-scan data. The MFL B-scans represent the data from a single sensor as it is being moved through the centres of the nearby pittings along the circumferential direction. MFL B-scans were used to estimate the depths of the pittings.

Estimation of the pitting depth from the MFL amplitude alone is difficult unless the area parameter (diameter) of the pitting is established first. The MFL signal is a unipolar signal and its amplitude is not directly proportional to the depth but more closely related to the volume of the defects. So, the depth can be extracted from the area (diameter) and volume (MFL signal amplitude) data of the defect. After the pitting diameter is estimated, its value together with the maximum amplitude of the corresponding MFL signal are utilised to estimate the pitting depth. These inputs are shown in "Fig. 15" as input 1 and input 2, respectively.

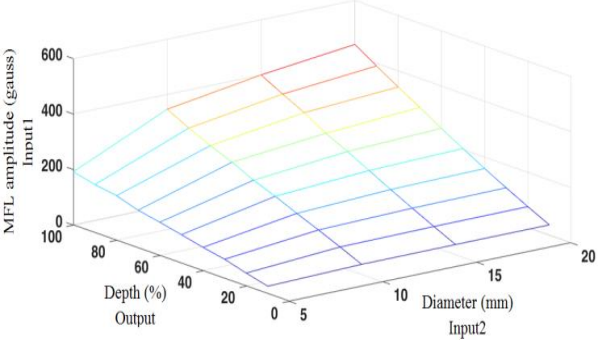

Fig. 15 Depth estimation of the pitting using the diameter and MFL signal amplitude data.

It should be noted that the calibration surface is produced with a reference set of pitting defects. In "Fig. 15", the peak amplitude of the MFL signals as a function of the pitting diameter and pitting depth is presented. The diameters of the pitting defects varied from 5mm to 20mm and the depths of them varied from 10% (1mm) to 100% (10mm). The peak amplitude of the MFL signal was acquired by subtracting the background signal from the total MFL signal. Using the appropriate interpolation and extrapolation method, this calibration surface can be used to identify the pittings with different diameters and depths.

Table 2 shows the diameter and depth estimation results compared to the real sizes of the pittings.

Table 2 The results of the diameter and depth estimations

The spacing between the pittings	Pitting depth	Pitting diameter (mm)	MFL amplitude (gauss)	Diameter error (mm)	Depth error (%)
4R=20mm	80%t	10	307	-0.013	2
	30%t	10	199	-0.033	22
3R=15mm	80%t	10	313	-0.01	5
	30%t	10	225	0.045	32
2R=10mm	80%t	10	327	-0.006	10
	30%t	10	248	-0.005	40
1R=5mm	80%t	10	341	-0.054	12
	30%t	10	292	0.001	51

The results show that the proposed combined approach provides good results for depth estimation of the deep pitting. However, the estimated depths differ somewhat from the real values. This can be explained by the fact that the calibration surface is produced with the single pitting. Nearby pittings may be considered as an area wherein the leakage fluxes coming from the nearby pittings interact with each other. The circumferential proximity of the pittings influences the absolute value of the MFL signals and increases them due to the superposition of the leakage fluxes.

When the separation distance between two pittings is too short, the MFL signals are superimposed strongly which results in depth overestimation particularly in case of the shallow pitting.

In the case of the deep pitting with a depth of 8mm, the highest depth estimation error was 12% for the separation distance of 1R (5mm). From Table 2, it is clear that significant overestimation of the depth occurred when the spacing between the defects reduced. It is a consequence of a higher superposition of the leakage fluxes coming from the nearby pittings in the case of a smaller separation distance.

When the separation distance of two pittings was 1R (5mm), the MFL signals superimposed strongly and depth estimation error was high. In this case, the depth estimation error of the shallow pitting with a depth of 3mm was 51%. When the separation distance increased to 4R (20mm), the leakage fluxes had little interaction with each other, and the depth estimation errors reduced. In this case, the errors were 2% and 22% respectively for the deep and shallow pitting with a separation distance of 20mm.

Understanding the effects of the separation distances of the nearby pittings on the leakage fluxes is very important in improving the accuracy and reliability of the MFL inspection technique. A better understanding of these factors permits effective compensation for the superposition of the leakage fluxes coming from the nearby pittings and will be beneficial for obtaining more accurate sizes of the defects.

6 CONCLUSION

One of the most challenging defects for traditional MFL technique is nearby pittings. This study has described a novel approach for detection and identification of the nearby pittings using the combination of MFL technique with optical inspection technique. The ultimate goal of this research work was to improve the depth estimation accuracy of the nearby pittings. In order to perform this experimental study, various nearby pittings were considered according to the distance between the single pittings. This type of defect geometry comprised two pittings that were vertically aligned to the magnetic field direction. MFL and optical inspection experiments were performed on the flat specimen with machined defects and their contributions to defect characterization were studied. Application of the MFL technique in combination with the optical inspection technique clearly showed that the combined approach provided an increased distinction of the individual pittings and therefore resulted in a better depth estimation of the pittings. Also, the results showed that the accuracy of the depth estimation reduced when decreasing the separation distance between the pittings. However, good results were obtained for the depth estimation of the deep pitting.

REFERENCES

[1] Gunaltun, Y., Top of Line Corrosion in Gas Lines Confirmed by Condensation Analysis, Oil & Gas Journal, Vol. 97, No. 28, 1999.

[2] Benjamin, A. C., Freire, J. L. F., and Vieira, R. D., Analysis of Pipeline Containing Interacting Corrosion Defects, Experimental Techniques, Vol. 31, No. 3, 2007, pp. 74-82.

[3] Silva, R. C. C., Guerreiro, J. N. C., and Drach, P. R. C., A Study on the Assessment and Interaction Criteria for Pipes Containing Multiple Corrosion Defects, Proceedings of the Rio pipeline conference, RPC 2009, 2009.

[4] Freire, J. L. F., Vieira, R. D., Fontes, P. M., Benjamin, A. C., Colquicocha, L. S. M., and Miranda, A.C., The Critical Path Method for Assessment of Pipelines with Metal Loss Defects, Proceedings of the 9th international pipeline conference, IPC 2012, 2012.

[5] Singer, M., CO2 Top of the Line Corrosion in Presence of Acetic Acid: A Parametric Study, Proceedings of NACE CORROSION, Paper No. 09292, Atlanta, 2009.

[6] Coramik, M., and Ege, Y., Discontinuity inspection in pipelines: A Comparison Review, Measurement, Vol. 111, 2017, pp. 359–373.

[7] Bai, Y., Pipelines and Risers, Elsevier Ocean Engineering Series Editors, USA, 2001.

[8] Suresh, V., Abudhahir, A., and Jackson, D., Development of Magnetic Flux Leakage Measuring System for Detection of Defect in Small Diameter Steam Generator Tube, Measurement, Vol. 95, 2017, pp. 273–279.

[9] Porter, P. C., Use of Magnetic Flux Leakage (Mfl) For The Inspection of Pipelines and Storage Tanks. Proceedings of the Nondestructive Evaluation of Aging Utilities, SPIE 2454, 1995, pp. 172–184.

[10] Feng, Q., Li, R., Nie, B., Liu, S., Zhao, L., and Zhang, H., Literature Review: Theory and Application of In-line Inspection Technologies for Oil and Gas Pipeline Girth Weld Defection, Sensors, Vol. 17, No. 50, 2017, pp. 1-24.

[11] Sutherland, J., and Paz, H., Advances in In-Line Inspection Technology for Pipeline Integrity, Proceedings of the 5th Annual International Pipeline Congress, Morelia, Mexico, 2000.

[12] Azizzadeh, T., and Safizadeh, M. S., Three-Dimensional Finite Element and Experimental Simulation of magnetic

flux leakage-type NDT for Detection of Pitting Corrosions, URL: http://www.NDT.net/article/ IranNDT2017/papers/520.pdf, February 2017.

[13] Huyse, L., Roodselaar, A. V., Onderdonk, J., Wimolsukpirakul, B., Baker, J., Beuker, T., Palmer, J., and Jemari , N. A., Improvements in the Accurate Estimation of Top of the Line Internal Corrosion of Subsea Pipelines on the Basis of In-Line Inspection Data, Proceedings of the 8th International Pipeline Conference, Calgary, Alberta, Canada, 2010, pp.1-8.

[14] Saunderson, D. H., The MFL Tank Floor Scanner - A Case History, Proceedings of the IEE colloquium on non-destructive evaluation, 1988.

[15] Joshi, A., Udpa, L., Udpa, S., and Tamburrino, A., Adaptive Wavelets for Characterizing Magnetic Flux Leakage Signals from Pipeline Inspection, IEEE Transaction on Magnetics, Vol. 42, No. 10, 2006, pp. 3168-3170.

[16] Haggag, F. M., Innovative Ssm Technology Determines Structural Integrity of Metallic Structures: Example Applications for Pressure Vessels and Oil and Gas Pipelines, International Journal of Pure and Applied Physics, Vol. 3, No. 1, 2007, pp. 91-108.

[17] Ji, F., Wang, C., Sun, S., and Wang, W., Application of 3-D FEM in the Simulation Analysis for MFL Signals, Insight: Non-Destructive Testing and Condition Monitoring, Vol. 51, No. 1, 2009.

[18] Saha, S., Mukhopadhyay, S., Mahapatra, U., Bhattacharya, S., and Srivastava, G. P., Empirical Structure for Characterizing Metal Loss Defects from Radial Magnetic Flux Leakage, NDT & E International, Vol. 43, 2010, pp. 507–512.

[19] Kin, J. H., Kim, M. H., and Choi, D. H., Analysis and Depth Estimation of Complex Defects on the Underground Gas Pipelines, Journal of magnetics, Vol. 18, No. 2, 2013, pp. 202-206.

[20] Niese, F., Yashan, A., and Willems, H., Wall-Thickness Measurement Sensor for Pipeline Inspection using EMAT Technology in Combination with Pulsed Eddy Current and MFL, Proceedings of the 9th European Conference on NDT, ECNDT 2006, Berlin, 2006, pp. 1-10.

[21] Jian, F., Feng, Z., Xiang, L., Yang, W., and Ze, M., Three-axis Magnetic Flux Leakage In-Line Inspection Simulation Based On Finite-Element Analysis, Chinese physical society, Vol. 22, No. 1, 2013, pp. 1-6.

[22] Lim, M. K., and Cao, H., Combining Multiple Ndt Methods to Improve Testing Effectiveness, Construction and Building Materials, 2011.

[23] Oagaro, J. A., and Mandayam, S., Multi-Sensor Data Fusion Using Geometric Transformations for Gas Transmission Pipeline Inspection, Proceedings of the IEEE International Instrumentation and Measurement Technology Conference, IMTC 2008, Victoria, Vancouver Island, Canada, 2008.

[24] Goller, C., Simek, J., and Ludlow, J., Multiple Data Set Ili for Mechanical Damage Assessment, Proceedings of the 9th International Pipeline Conference, IPC 2012, Calgary, Alberta, Canada, 2012, pp. 1-9.

[25] Safizadeh, M. S., and Azizzadeh, T., Corrosion Detection of Internal Pipeline using NDT Optical Inspection System, NDT & E International, Vol. 52, 2012, pp. 144–148.

[26] Qi, J., Qingmei, S., Nan, L., Paschalis, Z., and Jihong, W., Detection and Estimation of Oil-Gas Pipeline Corrosion Defects, Proceedings of the 18th international conference on systems engineering, ICSE 2006, 2006, pp. 173–177.

[27] Rostami Kandroodi, M., Shirani, F., Nadjar Araabi, B., Nili Ahmadabadi, M., and Mansoob Basiri, M., Defect Detection and Width Estimation in Natural Gas Pipelines using MFL Signals, Proceedings of the 9th Asian Control conference, Istanbul, Turkey, 2013, pp. 1–6.

[28] Zhang, Z., A Flexible New Technique ffor Camera Calibration, IEEE Transaction on Pattern Analysis and Machine Intelligence, Vol. 22, 2000, pp. 1330–1334.

[29] Gonzalez, R. C., Digital image processing, Addison - Wesley, Massachusetts, USA, 1987.

[30] Nestleroth, J. B., and Bubenik, T. A., Magnetic Flux Leakage Technology for Natural Gas Pipeline Inspection, Technical Report GRI-00/0180, Battelle, Topical Report to Gas Research Institute, February 1999.